

Cross-relaxation effects in the 2.818-eV zero-phonon emission in brown diamond

I. Hiromitsu,* J. Westra, and M. Glasbeek

Laboratory for Physical Chemistry, University of Amsterdam, Nieuwe Achtergracht 127, 1018 WS, Amsterdam, The Netherlands

(Received 27 January 1992)

In brown diamond, the long-lived emission at 2.818 eV is known to be due to a localized center in the photoexcited triplet state. In this paper, the emission intensity of the 2.818-eV center is studied as a function of the strength of an externally applied magnetic field. The cross-relaxation (CR) with $N-V$ centers, P_1 centers, and $g=2$ doublet spins of unknown origin, as well as level anticrossing (LAC), is found to affect the phosphorescence intensity for certain magnetic-field strengths and orientations. The CR dynamics is studied optically by measuring the phosphorescence transients induced by microwave pulses resonant with a spin transition in the photoexcited triplet state. Under CR conditions, spin population relaxation in the excited triplet state becomes faster and deviates from a single-exponential recovery behavior. The triplet-state kinetics including CR effects is studied theoretically, and a double-exponential recovery is predicted. Based on an analysis of the kinetics, the experimental microwave recovery transients under the CR conditions are satisfactorily simulated. The CR rate is estimated to be $(5.0 \pm 1.5) \times 10^2 \text{ s}^{-1}$ for the CR with the $N-V$ center and $(8.0 \pm 2.5) \times 10^2 \text{ s}^{-1}$ for the CR with the $g=2$ doublet species.

I. INTRODUCTION

Photoexcitation of a brown diamond sample at 364 nm gives rise to a long-lived luminescence with a zero-phonon line peaking at 441 nm (2.818 eV).¹ Recently, by means of optically detected magnetic resonance (ODMR) spectroscopy, it was shown² that the emission originates from an excited triplet state characterized by $g=2.00$, $|D|=924 \pm 2 \text{ MHz}$, and $|E|=198 \pm 2 \text{ MHz}$. The principal axes of the zero-field fine-structure tensor were found to be along the $[100]$, $[011]$, and $[01\bar{1}]$ axes of the diamond crystal,² showing the presence of a defect of rhombic- I symmetry,³ cf. Fig. 1(a). At 1.4 K, the lifetimes of the triplet-state sublevels, T_x , T_y , and T_z , are 0.5, 1.8, and 23 ms, respectively. The T_x level is the most emissive substate, whereas T_z is almost nonemissive. Under continuous optical excitation, a steady-state spin alignment is produced: the population of the T_x level is larger than for the other two sublevels [Fig. 1(b)]. Furthermore, the absence of the ODMR signal for the $|D|-|E|$ transition, i.e., the transition between the T_y and the T_z levels, indicates that the populations of these two sublevels are nearly equal.

In this paper, we report on cross-relaxation⁴ (CR) and level anticrossing^{4,5} (LAC) effects in the phosphorescence intensity of the 2.818-eV center for suitable values and orientations of an externally applied magnetic field. The basis for the experiments is that spin alignment becomes relaxed for those magnetic field strengths for which the triplet spins become resonant with other triplet or doublet defect spins [Figs. 1(c) and 1(d)], which are characterized by a spin temperature different from that of the probed 2.818-eV center triplet spins.

The dynamics of the CR processes is examined by means of time-resolved microwave recovery experiments performed for the 2.818-eV center in its photoexcited triplet state. In these experiments, the recovery of the

phosphorescence intensity is measured as a function of time after an initial microwave pulse has induced an ODMR transition. In Sec. II, it is analyzed how the triplet spin kinetics is affected by the CR. In Sec. IV, the experimental microwave recovery transients are simulated on the basis of the theoretical formulae obtained in Sec. II. From the computer fits, the CR rate can be estimated.

The detailed study of the CR processes provides a clear picture of the energy transfer processes that arise due to the magnetic dipole-dipole interaction occurring in the system. The present work also demonstrates that CR dynamics can be studied effectively by performing pulsed microwave recovery experiments.

II. ANALYSIS OF TRIPLET SPIN KINETICS IN THE PRESENCE OF CR

We consider a model consisting of four energy levels, the singlet ground state, and the excited triplet state. The equivalency of the four-level scheme to a more precise five-level scheme which includes the singlet excited state has been demonstrated elsewhere.⁶ In Fig. 2, the feeding and the decay rate constants of the triplet state are defined: A_i ($i=x,y,z$) represents the feeding rate, k_i^r the radiative decay rate, and k_i^n the nonradiative decay rate of the triplet sublevel, T_i . Neglecting spin-lattice relaxation, the rate equations for the populations of the four energy levels become⁷

$$\begin{aligned} \frac{dN_s}{dt} &= -(A_x + A_y + A_z)N_s + \sum_{j=x,y,z} K_j N_j, \\ \frac{dN_i}{dt} &= A_i N_s - K_i N_i \quad (i=x,y,z), \end{aligned} \quad (1)$$

where N_s and N_i represent the populations of the singlet state, S , and the triplet sublevel, T_i , respectively, and K_i is the total decay rate of the sublevel T_i defined by

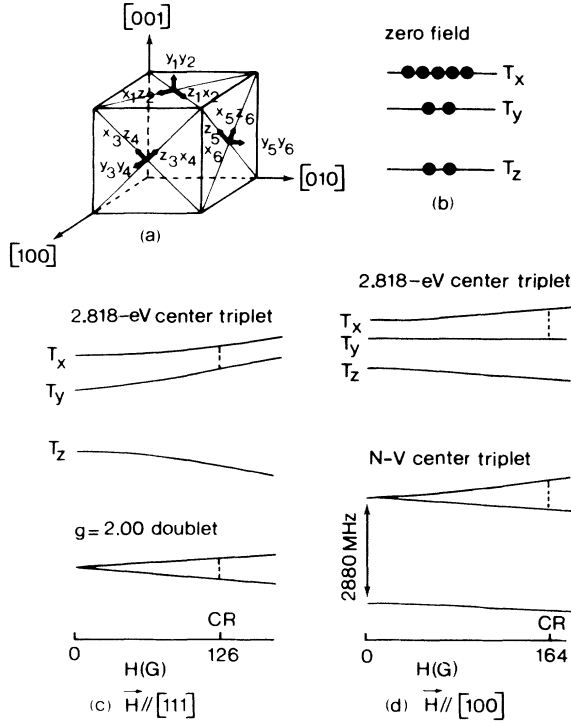


FIG. 1. (a) Orientation of the molecular axes of the six magnetically inequivalent sites of the 2.818-eV center with respect to the diamond crystallographic axes. (b) A schematic picture of the spin alignment of the 2.818-eV center triplet state at zero external magnetic field. (c) Magnetic-field dependences of the energies of the 2.818-eV center triplet sublevels for the magnetically equivalent sites 2, 4, and 6 and of a $g = 2.00$ doublet spin species, when the magnetic field is oriented along the $[111]$ crystal axis. CR between the two spin systems is energetically possible at 126 G. (d) Magnetic-field dependences of the 2.818-eV center triplet-state sublevel energies for the degenerate sites 3 and 4 and of the $N-V$ center triplet sublevel energies when the field is oriented along the $[100]$ crystal axis. CR is energetically possible at 164 G.

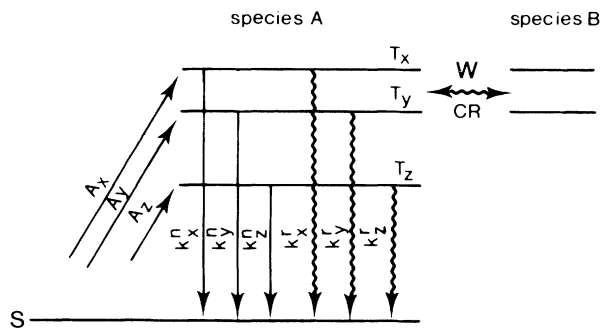


FIG. 2. A schematic representation of the energy levels of two species A and B which are resonant and show CR. The four energy levels of species A correspond to the singlet ground state (S) and the excited triplet state (T_x, T_y, T_z). $A_i, k_i^r,$ and k_i^n ($i = x, y, z$) represent feeding rate, radiative decay rate, and non-radiative decay rate, respectively, of the triplet sublevel T_i . Species B is resonant to the T_x to T_y sublevel transition. W represents the CR rate.

$K_i = k_i^r + k_i^n$. An additional condition,

$$N_s + \sum_{j=x,y,z} N_j = 1, \quad (2)$$

reduces the number of independent variables to three.

Now CR is taken into account explicitly. CR occurs when the energy difference between the sublevels T_x and T_y of a triplet spin species A is resonant with an energy difference of another spin species B . We assume that the species B forms a spin reservoir with a much larger heat capacity than species A . Furthermore, there is a fast energy transfer within the reservoir so that species B is always kept at a constant spin temperature identical to the lattice temperature, T . In this case, the rate equations become

$$\begin{aligned} \frac{d(N_x + N_y)}{dt} &= (A_x + A_y)N_s - K_x N_x - K_y N_y, \\ \frac{d(N_x - N_y)}{dt} &= (A_x - A_y)N_s - K_x N_x + K_y N_y \\ &\quad - W\{(N_x - N_y) - (N_x - N_y)_0\}, \quad (3) \end{aligned}$$

$$\frac{dN_z}{dt} = A_z N_s - K_z N_z,$$

where W is the CR rate and $(N_x - N_y)_0$ is the equilibrium value of $N_x - N_y$, i.e., when the spin temperature defined for the two sublevels T_x and T_y of species A becomes equal to that of the spin reservoir. With the present lattice temperature at 1.4 K, $(N_x - N_y)_0$ is approximately zero. In this case, Eq. (3) becomes

$$\frac{d}{dt} \mathbf{n} = \mathbf{A} - R \mathbf{n}, \quad (4)$$

where

$$\mathbf{n} = \begin{pmatrix} N_x \\ N_y \\ N_z \end{pmatrix}, \quad \mathbf{A} = \begin{pmatrix} A_x \\ A_y \\ A_z \end{pmatrix},$$

and

$$R = \begin{pmatrix} A_x + K_x + \frac{W}{2} & A_x - \frac{W}{2} & A_x \\ A_y - \frac{W}{2} & A_y + K_y + \frac{W}{2} & A_y \\ A_z & A_z & A_z + K_z \end{pmatrix}.$$

When the excitation laser power is not high enough to decrease the population of the singlet ground state significantly, as is approximately the case in our experiments, A_i ($i = x, y, z$) is much smaller than K_i and can be neglected in the matrix R .⁷ Then, Eq. (4) is easily solved, and the solutions are given by

$$\begin{aligned}
N_x(t) - N_x(\infty) &= \left[K_x + \frac{W}{2} - \lambda_- \right] C_+ e^{-\lambda_+ t} \\
&\quad + \frac{W}{2} C_- e^{-\lambda_- t}, \\
N_y(t) - N_y(\infty) &= -\frac{W}{2} C_+ e^{-\lambda_+ t} \\
&\quad + \left[\lambda_+ - K_y - \frac{W}{2} \right] C_- e^{-\lambda_- t}, \\
N_z(t) - N_z(\infty) &= D e^{-K_z t},
\end{aligned} \tag{5}$$

where

$$\lambda_{\pm} = \frac{1}{2} [(K_x + K_y + W) \pm \sqrt{(K_x - K_y)^2 + W^2}] \tag{6}$$

and C_{\pm} and D are integral constants determined by the initial conditions.

Now, in Sec. IV, two cases of microwave recovery experiments are considered. In case I, the microwave frequency is resonant with the energy difference between the T_x and the T_z sublevels, i.e., the $|D| + |E|$ ODMR transition. Also, as explained later, the emission from the T_x and the T_y sublevels in these experiments are detected with efficiencies of $\frac{2}{3}$ and $\frac{1}{3}$, respectively. One of the initial conditions in case I is then $N_y(0) = N_y(\infty)$ which leads to

$$\frac{C_+}{C_-} = \left[\lambda_+ - K_y - \frac{W}{2} \right] / \frac{W}{2} = \frac{W}{2} / \left[\lambda_+ - K_x - \frac{W}{2} \right].$$

The detected emission signal intensity in case I is then found to be

$$\begin{aligned}
I(t) &= \left[\frac{2}{3} k_x^r N_x(t) + \frac{1}{3} k_y^r N_y(t) \right] \times \text{const} \\
&= I(\infty) + C \left\{ \left[K_x - \lambda_- + \frac{W}{2} \left[1 - \frac{k_y^r}{2k_x^r} \right] \right] e^{-\lambda_+ t} \right. \\
&\quad \left. + \left[\lambda_+ - K_x - \left[1 - \frac{k_y^r}{2k_x^r} \right] \right] e^{-\lambda_- t} \right\},
\end{aligned} \tag{7}$$

where C is a constant.

In case II, the microwave frequency is resonant with the $T_x \rightarrow T_y$ transition ($2|E|$ ODMR transition), and the experiment is performed in such a way that only the emission from the T_y sublevel is detected with an efficiency of 1. An initial condition of case II is $N_x(0) + N_y(0) = N_x(\infty) + N_y(\infty)$, which implies

$$\frac{C_+}{C_-} = -\frac{\lambda_+ - K_y}{K_x - \lambda_-} = -\frac{\lambda_+ - K_x}{K_x - \lambda_-} \cdot \frac{W/2}{\lambda_+ - K_x - W/2}.$$

The detected emission signal intensity is then given as

$$\begin{aligned}
I(t) &= k_y^r N_y(t) \times \text{const} \\
&= I(\infty) + C' [(\lambda_+ - K_x) e^{-\lambda_+ t} \\
&\quad + (K_x - \lambda_-) e^{-\lambda_- t}],
\end{aligned} \tag{8}$$

where C' is a constant. Thus, in both cases I and II, a double-exponential microwave recovery is expected.

The signal intensities $I(t)$ in Eqs. (7) and (8) are determined by six parameters: K_x , K_y , W , k_y^r/k_x^r , C (C'), and $I(\infty)$. The values of K_x , K_y , and k_y^r/k_x^r have been determined independently by additional experiments to be discussed in Sec. IV. Thus, three unknown parameters, i.e., W , C (C'), and $I(\infty)$ are to be determined from Eqs. (7) and (8).

III. EXPERIMENT

The brown-colored diamond crystal is the same as used previously.² The crystal was mounted inside a slow-wave helix immersed in a pumped liquid-helium bath ($T = 1.4$ K). Optical excitation was at 364 nm using a cw Ar⁺-ion laser (Spectra Physics Series 2000) with 200-mW output power. The phosphorescence emitted perpendicular to the exciting light was focused on the entrance slit of a monochromator. Photodetection was at 490 nm using a GaAs photomultiplier tube HAMAMATSU R943-02. The ODMR spectrometer has been described elsewhere.⁸ The magnetic-field-induced change in the emission intensity⁴ was measured using 30-Hz amplitude modulation (10-G peak-to-peak) of the external magnetic field and applying phase-sensitive detection. The time-resolved microwave recovery of the emission intensity² was measured after a microwave pulse duration of typically 0.2 μ s in an external magnetic field. The pulse intensity corresponded to a Rabi frequency of about 3 MHz. The transient signal was accumulated on a PAR model 4202 signal averager.

IV. RESULTS

A. CR and LAC effects in the 2.818-eV phosphorescence

Figure 3 presents the derivative of the magnetic-field-induced changes in the phosphorescence intensity of the 2.818-eV center. The signal was obtained using 30-Hz amplitude modulation of the external magnetic field and applying phase-sensitive detection of the emission intensity.⁴ The field was applied parallel to the detection pathway which was perpendicular to the excitation light, and along either the [100] [Fig. 3(a)], [111] [Fig. 3(b)], or [011] [Fig. 3(c)] crystallographic directions. In Fig. 3, sudden changes in the emission intensity are observed at several magnetic-field strengths for each of the aforementioned crystallographic orientations. The angular variation of the field strengths of these signals is displayed by the dots in Fig. 4 upon rotation of the crystal about its [0 $\bar{1}$ 1] axis. Drawn curves represent the calculated field strengths at which CR is possible between the 2.818-eV center triplet spin and a $g = 2.00$ doublet spin (solid line) and between the 2.818-eV center triplet spin and $N-V$ center triplet spins^{4,9} (dashed line). A slight deviation of the rotation axis from the [0 $\bar{1}$ 1] direction of 2° was assumed in order to get the best agreement with experimental results.

First, the origin of the emission intensity change at 165 G along the [100] axis is examined. As is illustrated in Fig. 4, the angular dependence of the field strength for

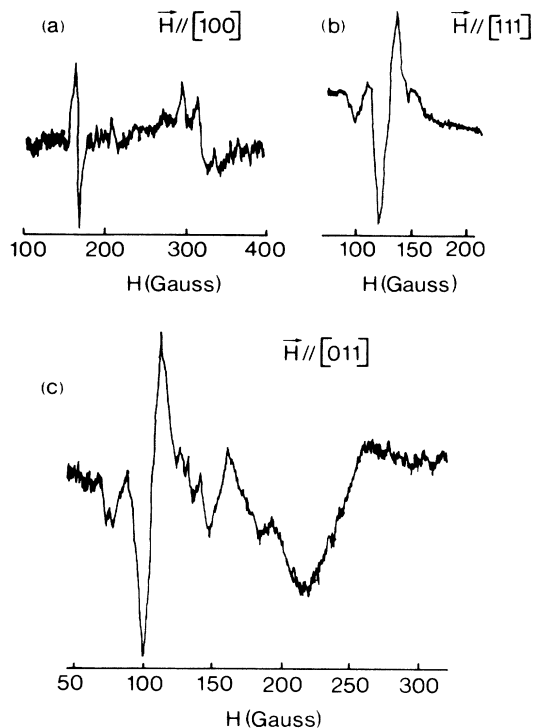


FIG. 3. Derivative of the phosphorescence intensity changes of the 2.818-eV center as induced by a magnetic field. The orientation of the magnetic field relative to the crystal axes is (a) $\vec{H} \parallel [100]$, (b) $\vec{H} \parallel [111]$, and (c) $\vec{H} \parallel [011]$. Detection wavelength: 490 nm; $T = 1.4$ K; amplitude modulation of the magnetic field is 10 G (peak-to-peak); phase-sensitive detection is at 30 Hz.

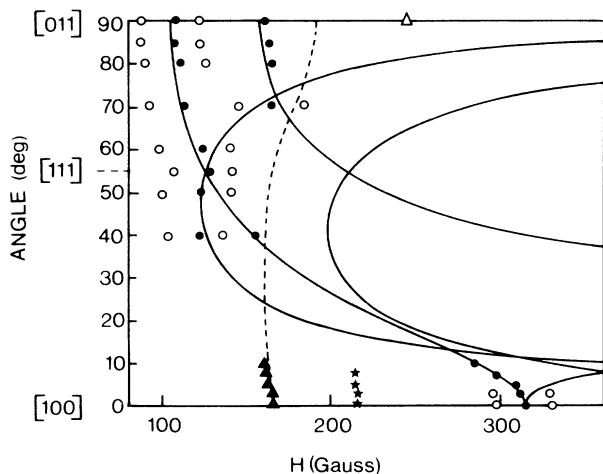


FIG. 4. Angular variation of the CR signals of Fig. 3 for rotation of the diamond crystal about the $[0\bar{1}1]$ axis perpendicular to the magnetic field. Experimental data include signals representative of CR between the 2.818-eV center and $g=2$ doublet spins (●) including hyperfine splittings (○) originated from the P_1 center, CR between the 2.818-eV center, and $N-V$ center triplet spins (▲), LAC (△). The origin of a weak signal represented by ★ is unknown. Drawn curves represent the calculated angular variation for the CR with the $g=2.00$ doublet (solid line) and the CR with the $N-V$ center triplet (dashed line). A misalignment of 2° was assumed in the calculation for the rotation axis from the $[0\bar{1}1]$ direction in order to get the best agreement with the experimental points.

rotation up to about 10° of this signal agrees well with the calculated one for the CR with the $N-V$ center triplet spin. No CR with $g=2.00$ doublet spins and no LAC are possible in this region. Thus, it is concluded that the signal at 165 G along $[100]$ axis is due to the CR between the 2.818-eV center excited triplet state and the $N-V$ center in its triplet state. In fact, from ESR and ODMR studies of the sample, it was verified that the $N-V$ centers are present. It is also remarked that, since the 364-nm laser light does not excite $N-V$ centers, the CR result provides us with independent additional evidence that the ground state of the $N-V$ center is a triplet state, in agreement with previous studies.^{9,10} The CR signal due to CR with the $N-V$ center was detected only when the magnetic-field direction is within 10° from the $[100]$ axis and its intensity is found to decrease rapidly when the magnetic field is rotated further away from the $[100]$ axis.

The emission intensity changes observed when the magnetic field has a strength of 315 G ($\vec{H} \parallel [100]$), or of 128 G ($\vec{H} \parallel [111]$) and 108 and 160 G when \vec{H} is along the $[011]$ direction, are attributed to CR with a doublet spin system with $g=2$. This is clearly seen from the good agreement between the observed and the calculated angular dependences in Fig. 4. The most abundant doublet spin generally occurring in diamond derives from the presence of P_1 centers which consist of single isolated nitrogen impurity atoms substitutional for carbon atoms. In ESR, the P_1 center is characterized by an isotropic g value of 2.00 (Refs. 11–13) and hyperfine splitting constants of $A_{\parallel} = 113.98$ MHz and $A_{\perp} = 81.34$ MHz. Also, the present CR results reveal a hyperfine interaction with $I=1$, the splitting between the lower and the higher field components being about 30 G, in agreement with the magnitude expected for the ^{14}N hyperfine coupling constant in P_1 center.⁴ Anisotropy in the P_1 -center hyperfine interactions, reported previously,⁴ is hidden in the CR signals measured here because of the large modulation amplitude (10 G peak-to-peak) used in the present experiment.

From a more careful examination of the hyperfine splittings in Fig. 3, it is noted that the splitting between the central line and the lower field hyperfine component is larger than the splitting between the central line and the higher field component. The asymmetric hyperfine splitting cannot be explained by consideration of the anisotropy in the P_1 -center hyperfine interactions, the magnitude of which has been determined before.⁴ Nuclear quadrupolar interactions in the P_1 center, the magnitude of which has been reported to be a few MHz,^{12,13} is too small to explain the present asymmetry. The asymmetry may be explained by assuming overlap with another CR signal due to the presence of another doublet spin species whose g value is a little smaller than $g=2.00$. The much stronger intensity of the central line as compared to the intensities of the lower and the higher hyperfine components in Figs. 3(b) and 3(c) supports this interpretation. The overlap with another CR signal has also been proposed elsewhere in discussing CR between the diamond $N-V$ and P_1 centers.¹⁴

The emission intensity change observed when the magnetic field is 240 G along the $[011]$ axis (cf., Fig. 4) is at-

tributed to LAC for a site whose molecular x axis is oriented parallel to the external magnetic field. The avoided crossing is confirmed by means of ODMR, when the latter is studied as a function of the magnetic-field strength. The results are shown in Fig. 5. The energy separation of the avoided crossing levels is about 70 MHz. This corresponds to the influence of the off-diagonal Zeeman interaction^{5,15} when the sample is misaligned by about 2° from the [011] axis.

B. Optically detected microwave recovery transients

Time-resolved microwave recovery experiments were performed in order to study the spin dynamics of the CR process in the present system. Since CR is an energy transfer process, it affects the triplet-state population kinetics. Generally speaking, the CR effect is seen on the microwave recovery transients if the CR rate is in the same order as or faster than the decay rates and the spin-lattice relaxation rates of the excited triplet sublevels. The triplet-state kinetics including the CR has been discussed in Sec. II.

First, the CR kinetics for H at 128 G and along the [111] axis, i.e., the CR with the $g=2$ doublet spins, is considered. The $|D|+|E|$ ODMR signal around this field consists of two components as shown in Fig. 6. The lower-frequency component comes from three degenerate sites 2, 4, and 6 in Fig. 1(a), and the higher-frequency component comes from sites 1, 3, and 5. A triplet-state energy calculation indicates that the lower-frequency component takes part in the CR with the $g=2$ doublet spins at 126 G [Fig. 1(c)]. A microwave recovery experi-

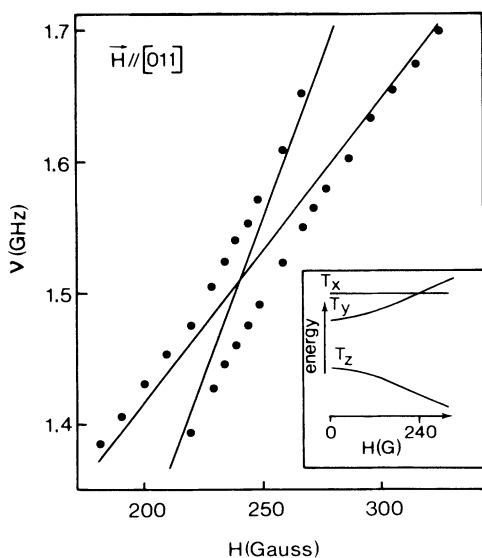


FIG. 5. $|D|+|E|$ and $|D|-|E|$ ODMR transition frequencies for site 4 of Fig. 1(a), for $\vec{H}||[011]$, and the field strength indicated in the figure, near the LAC region. The $|D|-|E|$ ODMR signal is detectable only at the LAC region. The solid lines show the calculated transition frequencies without taking into account the LAC effect. A misalignment of 2° from the exact [011] axis was assumed in the calculation. The inset shows the magnetic-field dependence of the triplet sublevel energies.

ment was performed by detecting the time dependence of the 2.818-eV center phosphorescence intensity after a $0.2\text{-}\mu\text{s}$ microwave pulse which is resonant to the lower-frequency ODMR transition. A schematic representation of the relevant directions in this experiment is shown in Fig. 7(a). The emissions from the T_x and the T_y levels are linearly polarized along the y and the x molecular axes, respectively,¹⁶ and the T_z level is almost nonemissive. The propagation efficiency of the emitted light to the direction of detection is determined by $\sin^2\vartheta$, ϑ being the angle between the polarization of the emitted light and the detection direction. After consideration of the contributions from sites 2, 4, and 6 in Fig. 7(a) to the linear polarization of the emitted light, the detection efficiencies of the emissions from the T_x and the T_y sublevels are obtained to be $\frac{2}{3}$ and $\frac{1}{3}$, respectively.

Figure 8 shows the microwave recovery transients with the magnetic-field strength outside (curve a) and inside (curve b) of the CR region. Curve a is fitted well by a single-exponential function with a decay rate of $1.3 \times 10^3 \text{ s}^{-1}$. This result is compatible with the decay constant of the T_x sublevel reported previously.² The experimental result is as expected because the microwave pulse resonant to the $|D|+|E|$ transition disturbs the populations of the T_z and the T_x sublevels, whereas the detection direction is such that the T_x -level emission change can be probed. In the CR region (curve b), the decay becomes faster. In order to see the influence of CR more clearly, the values of $\tau_{2/3}$ and $\tau_{1/3}$ are plotted in Fig. 9. $\tau_{2/3}$ and $\tau_{1/3}$ are defined in Fig. 8 as the times needed for the transient signal intensity to become $\frac{2}{3}$ and $\frac{1}{3}$ of the intensity at $t=0$. Similar plots of the $\tau_{2/3}$ and the $\tau_{1/3}$ values are also shown in Fig. 9 when the initial microwave pulse is resonant to the higher-frequency ODMR transition in Fig. 6. Note that the latter does not take part in the CR. Figure 9 clearly indicates that the CR makes the microwave recovery faster. It is also noted from Fig. 9 that the CR effect is larger for $\tau_{2/3}$ than for $\tau_{1/3}$. This means that the recovery transient in the CR region deviates from the single-exponential curve. Under the present experimental conditions, the double-exponential recovery Eq. (7) in Sec. II is expected. Since the values of K_x , K_y , and

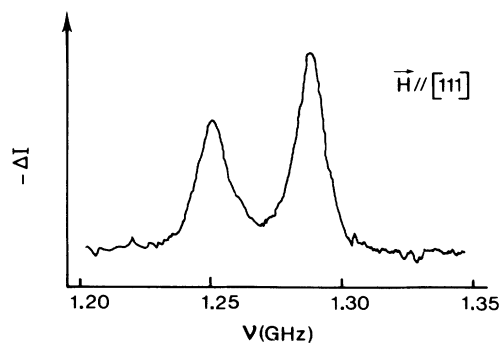


FIG. 6. $|D|+|E|$ ODMR signals of the 2.818-eV center phosphorescence with the external magnetic field of 117 G applied along the [111] crystal axis. $T=1.4 \text{ K}$. The 1.25-GHz signal is due to the degenerate sites 2, 4, and 6 of Fig. 1(a) and the 1.29-GHz signal is due to sites 1, 3, and 5.

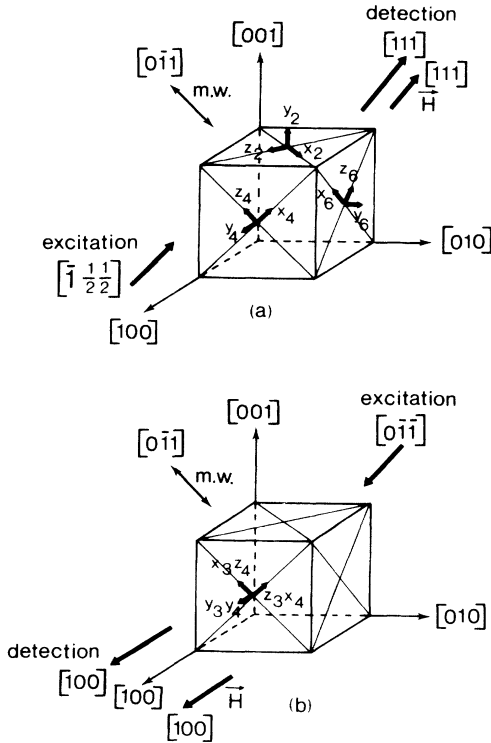


FIG. 7. Defect and crystal directions relevant to the microwave recovery experiments for (a) the CR of the 2.818-eV center with $g=2.00$ doublets, and (b) the CR of the 2.818-eV center with the $N-V$ center. m.w. indicates the direction of the linearly polarized microwave magnetic-field component.

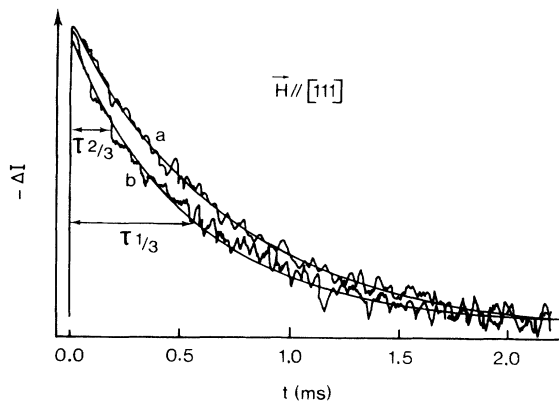


FIG. 8. Microwave recovery transients of the 2.818-eV center phosphorescence intensity after a $0.2\text{-}\mu\text{s}$ microwave pulse resonant to the $|D\rangle+|E\rangle$ transition of the magnetically equivalent sites 2, 4, and 6 of Fig. 7(a). *a*: The external magnetic field strength is 115 G (just outside of the CR region); *b*: 127 G (center of the CR region). $\mathbf{H}\parallel[111]$, $T=1.4\text{ K}$. $\tau_{2/3}$ and $\tau_{1/3}$ are defined as indicated in the figure. The drawn curve for *a* is a single-exponential curve with a decay constant of $1.3\times 10^3\text{ s}^{-1}$. The drawn curve for *b* is the best fit to Eq. (7) with $W=8.0\times 10^2\text{ s}^{-1}$. In the fitting procedure, the parameter values of K_x , K_y , and k'_y/k'_x in Eq. (7) were fixed to $1.4\times 10^3\text{ s}^{-1}$, $5.6\times 10^2\text{ s}^{-1}$, and 0.1, respectively.

k'_y/k'_x are known from the microwave recovery experiments outside the CR region, Eq. (7) includes only three unknown parameters, i.e., the CR rate W , the normalization factor C , and the offset $I(\infty)$. The microwave recovery transient in the center of the CR region is well fitted by Eq. (7). This is shown in Fig. 8(b) by the drawn line, which was calculated with a value of $W=(8.0\pm 2.5)\times 10^2\text{ s}^{-1}$. It is stressed that this fitting procedure includes only three unknown parameters, while normally a double-exponential fitting involves five unknown parameters. A similar double-exponential microwave recovery is observed in the CR region along the $[011]$ axis at 108 G, and the estimated CR time is $W=(9.0\pm 2.5)\times 10^2\text{ s}^{-1}$.

The CR between the 2.818-eV center excited triplet state and the $N-V$ center ground triplet state was also studied. In this case the microwave recovery experiment was performed with \mathbf{H} parallel to the $[100]$ direction. The schematic representation of the relevant directions in the experiment is given in Fig. 7(b). Sites 3 and 4 in Fig. 1(a) take part in the CR with the $N-V$ center at 165 G, and the microwave frequency was adjusted to the ODMR transition frequency for the transition involving the T_x and the T_y sublevels of these sites. With the scheme shown in Fig. 7(b), only the emission from the T_y sublevel is detected for sites 3 and 4 because the emission from the T_x sublevel is polarized along the detection direction. Outside the CR region, a single-exponential microwave recovery with a decay rate of about $5.6\times 10^2\text{ s}^{-1}$, which is identical with the decay rate of the T_y sublevel, was observed. This is as expected, since only the emission from

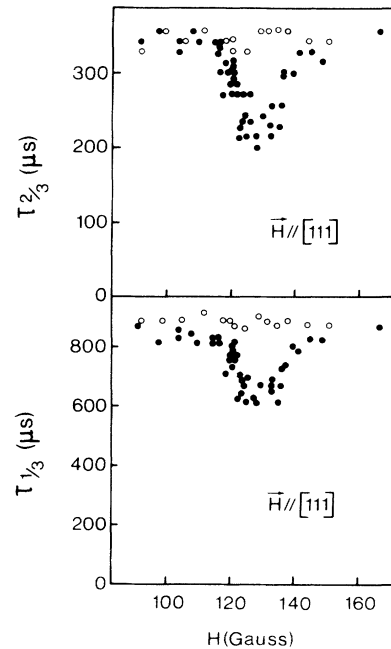


FIG. 9. $\tau_{2/3}$ and $\tau_{1/3}$ values of the microwave recovery transients as a function of magnetic field strength $\mathbf{H}\parallel[111]$. \bullet : for sites 2, 4, and 6 of Fig. 1(a), which take part in the CR with $g=2$ doublet spins at 126 G. \circ : for sites 1, 3, and 5, which do not take part in the CR process.

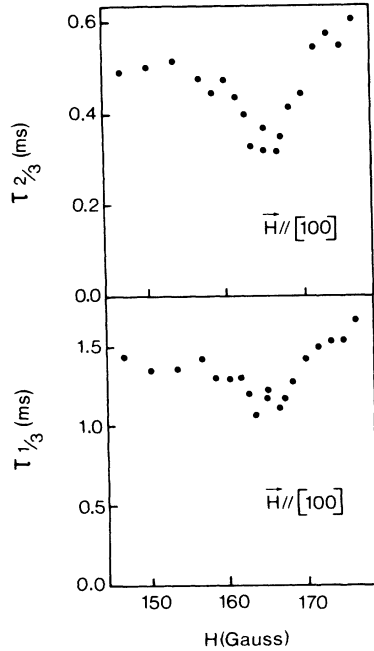


FIG. 10. $\tau_{2/3}$ and $\tau_{1/3}$ values of the microwave recovery transients as a function of magnetic field strength. $\vec{H}||[100]$. This is for sites 3 and 4 of Fig. 7(b), which take part in the CR with $N-V$ center at 165 G.

the T_y level is detected. In the CR region, a faster recovery was observed, as is clearly seen from the change of the $\tau_{2/3}$ and the $\tau_{1/3}$ values shown in Fig. 10. Again, the CR effect is larger for $\tau_{2/3}$ than for $\tau_{1/3}$, which is in agreement with the double-exponential recovery expected theoretically [Eq. (8)]. Equation (8) has three unknown parameters, W , C' , and $I(\infty)$. The experimental recovery transient in the center of the CR region is well fitted by Eq. (8) with $W = (5.0 \pm 1.5) \times 10^2 \text{ s}^{-1}$ as shown in Fig. 11.

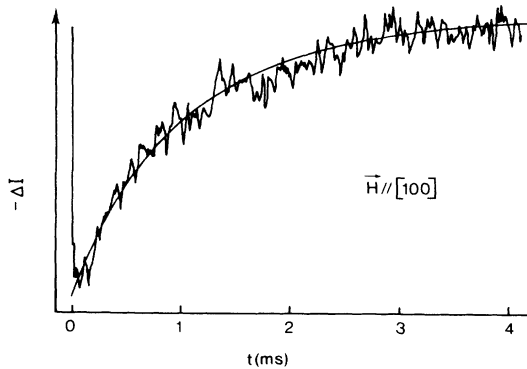


FIG. 11. Phosphorescence recovery transient for the 2.818-eV center after a $0.2\text{-}\mu\text{s}$ microwave pulse resonant to the $2|E|$ transition of sites 3 and 4 of Fig. 7(b). The drawn curve is the best fit to Eq. (8) with $W = 5.0 \times 10^2 \text{ s}^{-1}$. In the fitting procedure, the parameter values of K_x and K_y of Eq. (8) were fixed to 1.4×10^3 and $5.6 \times 10^2 \text{ s}^{-1}$, respectively.

V. DISCUSSION

From the results of the microwave recovery experiments presented in Sec. IV, a CR rate of $(5.0 \pm 1.5) \times 10^2 \text{ s}^{-1}$ was obtained for the CR between the photoexcited 2.818-eV center and the $N-V$ ground-state triplet spins, and a value of $(8.0 \pm 2.5) \times 10^2 \text{ s}^{-1}$ for the rate of CR between the 2.818-eV center triplet spins and the $g=2$ doublet spins. CR implies an energy transfer between two different spin systems, S_1 and S_2 . The process is caused by flip-flop (dynamic secular) terms of the type $S_1^+ S_2^- + S_1^- S_2^+$ (Ref. 17) of the magnetic dipole-dipole interaction. Because of the energy conservation law, these flip-flop terms are operative only when the two spin systems S_1 and S_2 are resonant. An alternative approach using a spin packet concept is that the CR between the two spin packets of the two spin species S_1 and S_2 is possible when the two spin packets have an overlap in their magnetic resonance frequencies. Because of this restriction, the CR becomes a much slower process as compared with the spin-spin relaxation caused by the static secular terms $S_1^z S_2^z$ (Ref. 17) of nonresonant dipole-dipole interactions with defects in the lattice containing an electron spin moment. In fact, the spin-spin relaxation rate of the 2.818-eV center triplet state is about $5 \times 10^4 \text{ s}^{-1}$, as determined from the measurement of the Hahn echo decay time.¹⁸ This relaxation rate is mainly determined by dipole-dipole interactions of the 2.818-eV center triplet state with spins located at surrounding $N-V$ centers, P_1 centers, and unknown doublet spins. The about 100 times slower CR process is reasonable if one compares the spin packet width of the 2.818-eV center triplet state with the inhomogeneous width of the surrounding spins, e.g., the $N-V$ center ensemble: The Hahn echo decay rate indicates that the spin packet width is in the order of 0.1 MHz, and the width of the CR region in Figs. 9 and 10 indicates that the inhomogeneous width is in the order of 10 MHz. Thus, about 1% of the surrounding spins can take part in the CR with one spin packet of the 2.818-eV center triplet spins, and, consequently, the CR rate of the latter is expected to differ from its homogeneous dephasing rate by approximately 2 orders of magnitude.

In the present emission intensity measurement, CR involving the triplet state of the 2.818-eV center and the P_1 -center doublet spins was detected, which is apparent from the existence of hyperfine splittings for the CR signals in Fig. 3. It is unlikely, however, that the CR with the P_1 center contributes to the change in the microwave recovery rate observed at the field 126 G along the [111] axis (Fig. 9). The arguments are as follows: (1) The CR region spreads more than 10 G in Fig. 9. Since an ESR study of the central line of the P_1 center indicates that its linewidth is smaller than 0.3 G,^{4,11} and the present microwave excitation spreads only 1 G at the center of the ODMR line of the triplet state, the region of the CR with the P_1 -center central line should not spread more than a few G. (2) The influence of hyperfine interaction of the P_1 center is not observed in Fig. 9. Thus, the detected CR effect in the microwave recovery experiment of Fig. 9 is tentatively assigned as due to the CR between the 2.818-eV center in the triplet state and the ensemble of

$g = 2$ doublet spins of unknown origin alluded to in Sec. IV A. This interpretation agrees with spin coherence experiments for the $N-V$ centers⁴ in which no CR effect has been detected for the CR between the $N-V$ center and the P_1 center. The lack of the CR effect with the P_1 center in the latter case was attributed to the very narrow P_1 -center linewidth compared to the microwave excitation width of about 1 G ($\cong 3$ MHz),⁴ as may also be the case in the present system.

Due to too weak signal intensities, no reliable spin coherence study was possible for the 2.818-eV center phosphorescence for external magnetic field values higher than 100 G. The results reported here illustrate that microwave recovery experiments provide a powerful alternative to spin coherence experiments in the study of CR dynamics.

VI. CONCLUSIONS

The phosphorescence intensity of the 2.818-eV center in brown diamond is affected by CR with $N-V$ centers, P_1 centers, and $g = 2$ doublet spins of unknown origin. In addition, the phosphorescence signal is also affected by LAC (Fig. 3). The results show that the degree of photoinduced spin alignment in the 2.818-eV center triplet state is changed due to CR and LAC processes. CR dynamics was studied by performing time-resolved mi-

crowave recovery experiments. The microwave recovery becomes faster when CR occurs (Figs. 8–10) in agreement with a kinetic analysis [Eqs. (7) and (8)]. The experimental microwave recovery transients were computer simulated with only three unknown parameters, and the CR rate, W , was estimated to be $(5.0 \pm 1.5) \times 10^2 \text{ s}^{-1}$ for the CR with the $N-V$ center and $(8.0 \pm 2.5) \times 10^2 \text{ s}^{-1}$ for the CR with unknown $g = 2$ doublet species. CR with the P_1 center is not detected in the microwave recovery experiment because of the very narrow width of the P_1 -center ESR signal. The CR rate is 2 orders of magnitude slower than the spin-spin relaxation rate of about $5 \times 10^4 \text{ s}^{-1}$. The order-of-magnitude difference is related to the fact that, in the CR process, the interacting spin systems must be resonant, whereas this constraint does not hold in the homogeneous spin dephasing mechanism.

ACKNOWLEDGMENTS

We thank Dr. R. T. Harley of The University of Southampton (UK) for providing the diamond crystal. This work was supported in part by the Netherlands Foundation for Chemical Research (SON) with financial aid from the Netherlands Organization for Scientific Research (NWO). One of the authors (I.H.) was supported in part by the Japanese Ministry of Education for his stay in Amsterdam.

*Permanent address: Physics Department, Shimane University, Matsue 690, Japan.

¹E. Pereira and L. Santos, *J. Lumin.* **40&41**, 139 (1988).

²J. Westra, R. Sitters, and M. Glasbeek, *Phys. Rev. B* **45**, 5699 (1992).

³A. A. Kaplyanskii, *Opt. Spectrosc.* **16**, 329 (1963).

⁴E. van Oort and M. Glasbeek, *Phys. Rev. B* **40**, 6509 (1989).

⁵W. M. Chen, M. Godlewski, and B. Monemar, and J. P. Bergman, *Phys. Rev. B* **41**, 5746 (1990).

⁶I. Hiromitsu and L. Kevan, *J. Chem. Phys.* **88**, 691 (1988).

⁷H. Levanon and S. Vega, *J. Chem. Phys.* **61**, 2265 (1974).

⁸M. Glasbeek and R. Hond, *Phys. Rev. B* **23**, 4220 (1981).

⁹E. van Oort, N. B. Manson, and M. Glasbeek, *J. Phys. C* **21**, 4385 (1988).

¹⁰N. R. S. Reddy, N. B. Manson, and E. R. Krausz, *J. Lumin.* **38**, 46 (1987).

¹¹W. V. Smith, P. P. Sorokin, I. L. Gelles, and G. J. Lasher, *Phys. Rev.* **115**, 1546 (1959).

¹²R. J. Cook and D. H. Whiffen, *Proc. R. Soc. London, Ser. A* **295**, 99 (1966).

¹³J. H. N. Loubser and L. du Preez, *Brit. J. Appl. Phys.* **16**, 457 (1965).

¹⁴E. van Oort, Ph.D. thesis, University of Amsterdam, 1990.

¹⁵E. van Oort and M. Glasbeek, *Chem. Phys.* **152**, 365 (1991).

¹⁶I. Hiromitsu, J. Westra, and M. Glasbeek (unpublished).

¹⁷A. Abragam, *The Principles of Nuclear Magnetism* (Clarendon, Oxford, 1961), Chap. IV.

¹⁸J. Westra, I. Hiromitsu, and M. Glasbeek (unpublished).